

# HIGHER-ORDER ORGANIZATION IN THE HUMAN BRAIN FROM MATRIX-BASED RÉNYI'S ENTROPY

Qiang Li<sup>1,5\*</sup>, Student Member, IEEE, Shujian Yu<sup>2†</sup>, Kristoffer H Madsen<sup>3,4</sup>, Vince D Calhoun<sup>5</sup>, Armin Iraj<sup>5</sup>

<sup>1</sup>Image Processing Laboratory, University of Valencia, Spain

<sup>2</sup>Department of Computer Science, Vrije Universiteit Amsterdam, The Netherlands

<sup>3</sup>Department of Applied Mathematics and Computer Science, Technical University of Denmark, Denmark

<sup>4</sup>Danish Research Centre for Magnetic Resonance, Copenhagen University Hospital, Denmark

<sup>5</sup>Tri-Institutional Center for Translational Research in Neuroimaging and Data Science (TReNDS), USA

## ABSTRACT

Pairwise metrics are often employed to estimate statistical dependencies between brain regions, however they do not capture higher-order information interactions. It is critical to explore higher-order interactions that go beyond paired brain areas in order to better understand information processing in the human brain. To address this problem, we applied multivariate mutual information, specifically, *Total Correlation* and *Dual Total Correlation* to reveal higher-order information in the brain. In this paper, we estimate these metrics using matrix-based *Rényi's entropy*, which offers a direct and easily interpretable approach that is not limited by direct assumptions about probability distribution functions of multivariate time series. We applied these metrics to resting-state fMRI data in order to examine higher-order interactions in the brain. Our results showed that the higher-order information interactions captured increase gradually as the interaction order increases. Furthermore, we observed a gradual increase in the correlation between the *Total Correlation* and *Dual Total Correlation* as the interaction order increased. In addition, the significance of *Dual Total Correlation* values compared to *Total Correlation* values also indicate that the human brain exhibits synergy dominance during the resting state.

**Index Terms**— Higher-order Interactions, Total Correlation, Dual Total Correlation, Rényi's Entropy, Resting State

## 1. INTRODUCTION

The brain is densely interconnected to facilitate efficient information transfer. The brain can be modeled as a fractal, chaotic, and complex system [1], and our understanding of the brain requires studying how higher-order information is distributed via networks at different levels (e.g., microscopic versus macroscopic, where we are concerned with the latter in this study).

Higher-order information enables intricate interactions among brain regions, these interactions encompass not only paired connections across brain regions, but also connections between three or more regions, as well as more complex and dynamic activity patterns including synchronization and phase relationships [2]. Furthermore, comprehending higher-order functional interactions is essential for understanding how the brain performs complicated activities and identifying biomarkers that can lead to improved diagnosis and treatment of neurological and psychiatric disorders [3, 4].

There are two general categories to investigate higher-order information interactions in the brain. The first category estimates higher-order interaction among brain networks using a hypergraph representation [5, 6]. The second category is information-theoretic approaches and uses the information shared across regions to estimate high-order interactions [3, 7, 8, 9]. Our focus in this paper is primarily on the latter approach, which aims to reveal higher-order information interactions in the human brain via information theory. For this purpose, we will use the two most commonly used metrics: (1) *Total Correlation (TC)* [10] (also known as *multi-information* [11] or *redundancy* [12]) and (2) *Dual Total Correlation (DTC)* [13] (also known as *binding information* [14] or *excess entropy* [15]).

There are various ways to estimate *TC* and *DTC*. One popular method is the Gaussian copula transform [16], which involves transforming non-Gaussian distributed multivariate time series into a Gaussian distribution based on a *copula transform* and then estimating the above metrics from their covariance [16]. However, in practice this method may face a range of challenges, for example, the power of these methods relies on the fact that the underlying fMRI BOLD signals can be well modeled by multivariate Gaussian distributions and thus allow efficient, easy, and analytically tractable estimation [17]. However, the use of this kind of processing ignores non-Gaussian distributed signals and does not provide a universal way to estimate them.

In this study, we used a more comprehensive approach, a

\*Corresponding author: qiang.li@uv.es

†Corresponding author: s.yu3@vu.nl

matrix-based *Rényi's entropy* for estimating higher-order information interactions and quantifying information organization in the human brain. Matrix-based *Rényi's entropy* [18, 19] estimates information in data without the need to know the underlying data distribution. This is achieved by utilizing the eigenspectrum of symmetric positive semi-definite matrices in a reproducing kernel Hilbert space. In our study, we investigate how higher-order information interactions can be captured by considering interaction orders beyond pairwise brain regions. Our specific interest lies in examining how the differences between *TC* and *DTC* vary as the interaction order increases, and how these metrics relate to the role of higher-order information in resting-state brain functions.

## 2. METHODOLOGY

### 2.1. Rényi's $\alpha$ entropy functional

In information theory, a natural extension of the well-known *Shannon's entropy* [20] is the *Rényi's  $\alpha$  entropy* [21]. For a random variable  $X$  with probability density function  $p(x)$  in a finite set  $\mathcal{X}$ , the  $\alpha$  entropy is defined as:

$$\mathbf{H}_\alpha(X) = \frac{1}{1-\alpha} \log \left( \int_{\mathcal{X}} p^\alpha(x) dx \right), \quad (1)$$

with  $\alpha \neq 1$  and  $\alpha \geq 0$ . In the limiting case where  $\alpha \rightarrow 1$ , it reduces to *Shannon's entropy* [22].

In practice, given  $m$  realizations sampled from  $p(x)$ , i.e.,  $\{x_i\}_{i=1}^m$ , Sanchez Giraldo *et al.* [23] suggests that one can evaluate  $\mathbf{H}_\alpha(X)$  without estimating  $p(x)$ . Specifically, the so-called *matrix-based Rényi's  $\alpha$  entropy* is given as:

$$\mathbf{H}_\alpha(X) = \frac{1}{1-\alpha} \log(\text{tr}(A^\alpha)), \quad (2)$$

where  $A \in \mathbb{R}^{m \times m}$  is a (normalized) Gram matrix with elements  $A_{ij} = K_{ij}/\text{tr}(K)$ ,  $K_{ij} = \kappa(x_i, x_j)$  in which  $\kappa$  stands for a positive definite and infinitely divisible kernel such as Gaussian.  $\text{tr}(\cdot)$  refers to matrix trace. As in [18], we set  $\alpha = 1.01$  to approximate Shannon entropy and choose a Gaussian kernel  $G_\sigma$  with width  $\sigma$ , given by,

$$G_\sigma(x_i, x_j) = \beta \exp \left( -\frac{\|x_i - x_j\|^2}{2\sigma^2} \right), \quad (3)$$

where  $\beta$  is a constant whose value is irrelevant because it is canceled out in the normalized Gram matrix.

Suppose now we have  $n \geq 2$  variables  $(X^1, X^2, \dots, X^n)$  and a collection of  $m$  samples<sup>1</sup>, i.e.,  $\{x_i^1, x_i^2, \dots, x_i^n\}_{i=1}^m$ , the *matrix-based Rényi's  $\alpha$  joint entropy* for  $n$  variables can be

<sup>1</sup>Throughout this paper, we use superscript to denote variable index and subscript to denote sample index. For example,  $x_i^3$  refers to the  $i$ -th sample from the 3rd variable.

evaluated as [18]:

$$\begin{aligned} \mathbf{H}_\alpha(X^1, X^2, \dots, X^n) &= \mathbf{H}_\alpha \left( \frac{K^1 \circ K^2 \circ \dots \circ K^n}{\text{tr}(K^1 \circ K^2 \circ \dots \circ K^n)} \right) \\ &= \frac{1}{1-\alpha} \log \left( \text{tr} \left( \left( \frac{K^1 \circ K^2 \circ \dots \circ K^n}{\text{tr}(K^1 \circ K^2 \circ \dots \circ K^n)} \right)^\alpha \right) \right), \end{aligned} \quad (4)$$

where  $(K^n)_{ij} = \kappa(x_i^n, x_j^n) \in \mathbb{R}^{m \times m}$  is a Gram matrix evaluated with  $\kappa$  for the  $n$ -th variable. The operator  $\circ$  is the Hadamard product.

### 2.2. Bivariate dependencies from *Mutual Information*

Bivariate dependencies can be inferred from *mutual information*, and if two variables are directly dependent, then the values are zeros. Given Eqs. 2 and 4, the *Rényi's  $\alpha$  entropy mutual information*  $\mathbf{I}_\alpha(X^1, X^2)$  between variables  $X^1$  and  $X^2$  in analogy of *Shannon's mutual information* is given by:

$$\mathbf{I}_\alpha(X^1; X^2) = \mathbf{H}_\alpha(X^1) + \mathbf{H}_\alpha(X^2) - \mathbf{H}_\alpha(X^1, X^2). \quad (5)$$

*Mutual information* is the most widely used metric for quantifying statistical dependency between two variables [22], but since it omits higher-order interactions in the system it does not capture all global information in the system.

### 2.3. Inferring higher-order dependencies through *Matrix-based Rényi's $\alpha$ TC and DTC*

The *TC* and *DTC* describe the dependence among  $n$  variables and can be considered as a non-negative generalization of the concept of *mutual information* from two parties to  $n$  parties. The definition of *TC* can be denoted as follows [10]:

$$\mathbf{T}(X^1, X^2, \dots, X^n) = \sum_{i=1}^n \mathbf{H}(X^i) - \mathbf{H}(X^1, X^2, \dots, X^n). \quad (6)$$

Analogously with *TC*, *DTC* can be defined as [13],

$$\begin{aligned} \mathbf{D}(X^1, X^2, \dots, X^n) &= \mathbf{H}(X^1, X^2, \dots, X^n) - \sum_{i=1}^n \mathbf{H}(X^i | X^{[n] \setminus i}) \\ &= \left[ \sum_{i=1}^n \mathbf{H}(X^{[n] \setminus i}) \right] - (n-1) \mathbf{H}(X^1, X^2, \dots, X^n), \end{aligned} \quad (7)$$

where  $X^{[n] \setminus i} = \{X^1, X^2, \dots, X^{i-1}, X^{i+1}, \dots, X^n\}$ , i.e., the set of all variables excluding  $X^i$ . From these definitions in Eqs. 6, 7, if all variables are independent, both *TC* and *DTC* will be zero. Beyond this, *TC* and *DTC* are closely related,

$$\mathbf{D}(X^1, X^2, \dots, X^n) \leq (n-1) \mathbf{T}(X^1, X^2, \dots, X^n). \quad (8)$$

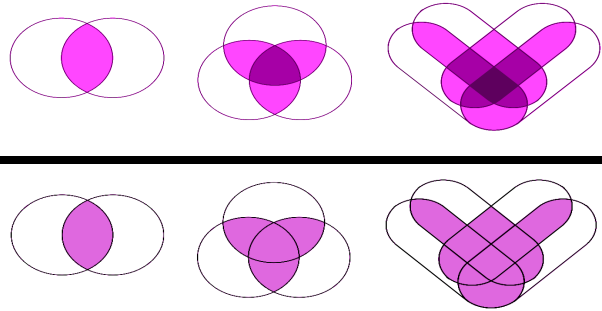


**Fig. 1: Information diagrams for  $TC$  (top) and  $DTC$  (bottom).** The top depicts the information interaction of 2-variable, 3-variable, and 4-variable measures from  $TC$ , while the bottom depicts the information interaction of 2-variable, 3-variable, and 4-variable measures from  $DTC$ . For a 3-variable case, the deep purple indicates information duplicated twice, the light purple indicates information duplicated once, and so on for a 4-variable situation.

In cases 2-variable, 3-variable, and 4-variable, the venn diagrams (see Fig. 1) provide a graphical representation of  $TC$  and  $DTC$ .

In order to estimate  $TC$  and  $DTC$  in a practical setting only from  $m$  samples  $\{x_i^1, x_i^2, \dots, x_i^n\}_{i=1}^m$ , we convert Eqs. 6 and 7 to matrix-based *Rényi's  $\alpha$  entropy functional* based on Eqs. 2 and 4, which simplifies the estimation [18, 19] and enables a reformulation:

$$\begin{aligned} \mathbf{T}_\alpha(X^1, X^2, \dots, X^n) &= \sum_{i=1}^n \mathbf{H}_\alpha(X^i) - \mathbf{H}_\alpha(X^1, X^2, \dots, X^n) \\ &= \left[ \sum_{i=1}^n \frac{1}{1-\alpha} \log \left( \text{tr} \left( \frac{K^i}{\text{tr}(K^i)} \right)^\alpha \right) \right] \\ &\quad - \frac{1}{1-\alpha} \log \left( \text{tr} \left( \left( \frac{K^1 \circ K^2 \circ \dots \circ K^n}{\text{tr}(K^1 \circ K^2 \circ \dots \circ K^n)} \right)^\alpha \right) \right), \end{aligned} \quad (9)$$

$$\begin{aligned} \mathbf{D}_\alpha(X^1, X^2, \dots, X^n) &= \left[ \sum_{i=1}^n \mathbf{H}_\alpha \left( X^{[n] \setminus i} \right) \right] \\ &\quad - (n-1) \mathbf{H}_\alpha(X^1, X^2, \dots, X^n). \end{aligned} \quad (10)$$

If  $\mathbf{D}_\alpha > \mathbf{T}_\alpha$ , the system becomes synergistic and dominant, while the system becomes redundancy dominant in the opposite case [7].

### 3. EXPERIMENTS

#### 3.1. Higher-order information in the human brain

##### 3.1.1. HCP dataset

The preprocessed time series obtained from rsfMRI data were utilized in [24]. For details regarding the scanning parameters

and related preprocessing for both structural and functional MRI, refer to [24]. After preprocessing, each subject was represented by a set of 116 time series of rsfMRI signals, consisting of 1200 samples with a repetition time of 720 ms, each corresponding to a specific region of interest. To limit the computational complexity, we randomly selected 10 subjects that were not related and applied multivariate information-theoretic metrics to quantify high-order information interaction in the brain.

##### 3.1.2. Brain atlas and interaction order

The whole brain was divided into 116 brain areas using the AAL116 brain atlas [25]. Considering the excessive computational cost, we limited our examination of the interaction order to only 2, 3, and 4 brain regions. Fig. 2 presents the general framework, and the left panel shows the AAL116 regions (with nodes representing the 116 brain regions and their corresponding time series) mapped to the Colin27 smoothed brain surface template [26]. The different brain lobes are labeled on the brain surface with different colors. The right panel is a representation of multiple interaction orders in the brain, such as interaction orders 2, 3, and 4. The green node indicates brain regions, and the number,  $N=1, 2, \dots, 116$  is the index for brain regions.

## 4. CONCLUSIONS AND FUTURE WORK

We present a matrix-based approach to estimate higher-order information using *Rényi's entropy*, which provides a more simplified method for quantifying such information. We further quantified higher-order information using resting-state fMRI as presented in Figure 3, where  $TC$  and  $DTC$  were utilized. It is evident from the plots and the second-order polynomial fits that  $TC$  and  $DTC$  are equivalent ( $R^2=1.00$ ) because they both represent *mutual information* at interaction order 2. However, with interaction orders exceeding 2 (e.g., 3 and 4), higher-order information is captured, and as the interaction order increases, the correlation between  $TC$  and  $DTC$  increases (e.g.,  $R^2=0.57, 0.68$ ), and  $DTC$  is greater than  $TC$  (as shown in the first row). Furthermore, the average  $TC$  and  $DTC$  for 10 subjects are represented for each interaction order in the second row middle Figure 3, and when we combined all interaction orders together (as shown in the second row, right panel), our finding that  $DTC$  is more significant than  $TC$  ( $p<0.05$ ) in resting-state brain activity suggests that synergy is dominant during resting-state situations in the human brain due to default mode networks, which is consistent with previous findings [27].

Here, we initially limited our analysis to interaction orders of 2, 3, and 4 due to computational constraints. However, it would be intriguing to investigate higher interaction orders in future research. Secondly, from a technical perspective,  $TC$  and  $DTC$ , can also be used to estimate redundancy and synergy, respectively [7]. It will be an important next goal to extend

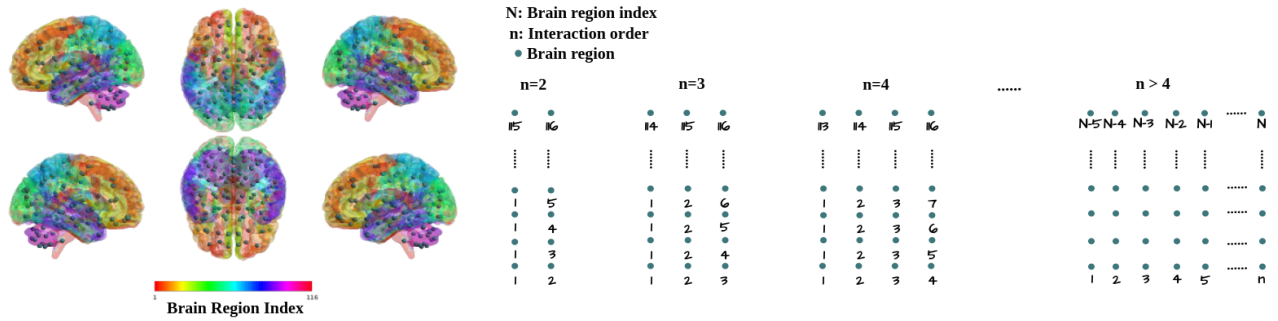


**Fig. 2: Brain parcellation and possible interaction order in the brain.** The left side is the AA116 brain atlas, and the right side is the various interaction orders in the human brain. For more information, see Section 3.1.2.

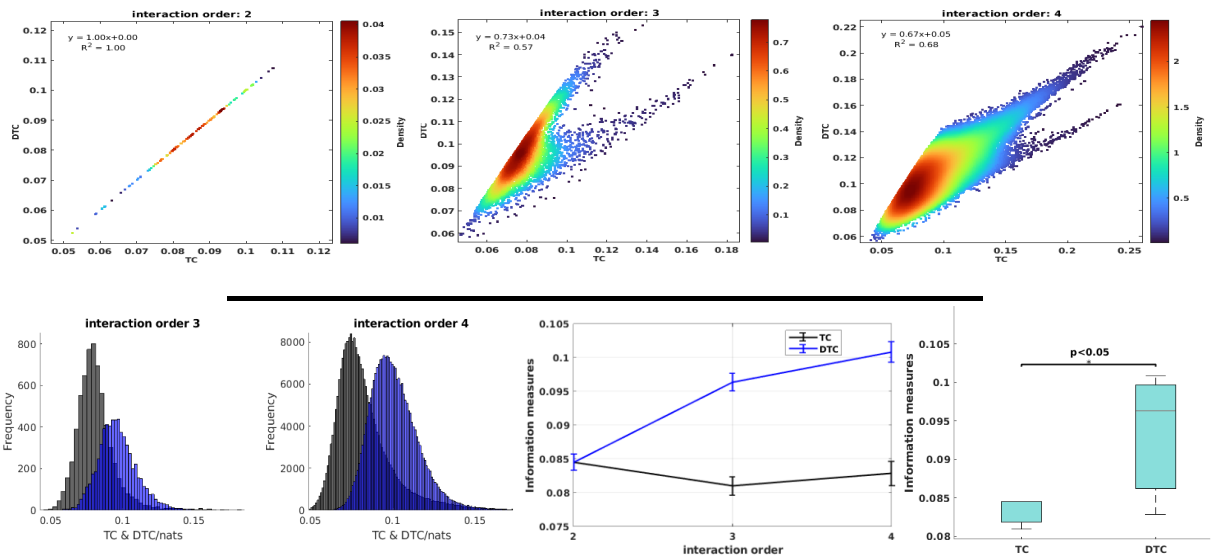


**Fig. 3: Higher-order information interaction in the brain.** The upper panels illustrate how the brain represents higher-order information under resting state, at increasing interaction orders of 2, 3, and 4. The lower panels presented some related statistical tests. For further details, please refer to the explanation provided in the conclusion section.

this research to investigate these aspects further. Thirdly, in terms of practical applications, it is promising to use these information-theoretical metrics to quantify changes in higher-order information interaction in major brain disorders and to extend the investigations to multiple modalities. Fourthly, using more large and task-related fMRI datasets to test the above conclusion would be very interesting in future work, and even more, considering the computation complexity for higher-order brain region interaction, we should consider using independent component networks instead of regions of interest.

## 5. REFERENCES

[1] Larry S Liebovitch, *Fractals and chaos simplified for the life sciences / Larry S. Liebovitch.*, Oxford University Press, New York, 1998.

[2] Fran Hancock, Joana Cabral, Andrea I Luppi, Fernando E

Rosas, Pedro AM Mediano, Ottavia Dipasquale, and Federico E Turkheimer, “Metastability, fractal scaling, and synergistic information processing: what phase relationships reveal about intrinsic brain activity,” *NeuroImage*, vol. 259, pp. 119433, 2022.

[3] Qiang Li, Greg Ver Steeg, Shujian Yu, and Jesus Malo, “Functional connectome of the human brain with total correlation,” *Entropy*, vol. 24, no. 12, pp. 1725, 2022.

[4] Rubén Herzog, Fernando E Rosas, Robert Whelan, Sol Fittipaldi, Hernando Santamaria-Garcia, Josephine Cruzat, Agustina Birba, Sebastian Moguilner, Enzo Tagliacuzzi, Pavel Prado, et al., “Genuine high-order interactions in brain networks and neurodegeneration,” *Neurobiology of Disease*, vol. 175, pp. 105918, 2022.

[5] Federico Battiston, Giulia Cencetti, Iacopo Iacopini, Vito Latora, Maxime Lucas, Alice Patania, Jean-Gabriel

- Young, and Giovanni Petri, “Networks beyond pairwise interactions: structure and dynamics,” *Physics Reports*, vol. 874, pp. 1–92, 2020.
- [6] Andrea Santoro, Federico Battiston, Giovanni Petri, and Enrico Amico, “Higher-order organization of multivariate time series,” *Nature Physics*, pp. 1–9, 2023.
- [7] Fernando E Rosas, Pedro AM Mediano, Michael Gastpar, and Henrik J Jensen, “Quantifying high-order interdependencies via multivariate extensions of the mutual information,” *Physical Review E*, vol. 100, no. 3, pp. 032305, 2019.
- [8] Qiang Li, “Functional connectivity inference from fmri data using multivariate information measures,” *Neural Networks*, vol. 146, pp. 85–97, 2022.
- [9] Qiang Li, Greg Ver Steeg, and Jesus Malo, “Functional connectivity in visual areas from total correlation,” *arXiv preprint arXiv:2208.05770*, 2022.
- [10] Satoshi Watanabe, “Information theoretical analysis of multivariate correlation,” *IBM Journal of research and development*, vol. 4, no. 1, pp. 66–82, 1960.
- [11] Milan Studený and Jirina Vejnarová, “The multiinformation function as a tool for measuring stochastic dependence.,” *Learning in graphical models*, vol. 89, pp. 261–297, 1998.
- [12] Han Te Sun, “Multiple mutual informations and multiple interactions in frequency data,” *Inf. Control*, vol. 46, pp. 26–45, 1980.
- [13] Te Sun Han, “Nonnegative entropy measures of multivariate symmetric correlations,” *Inf. Control*, vol. 36, no. 2, pp. 133–156, 1978.
- [14] Vikram S Vijayaraghavan, Ryan G James, and James P Crutchfield, “Anatomy of a spin: the information-theoretic structure of classical spin systems,” *Entropy*, vol. 19, no. 5, pp. 214, 2017.
- [15] Ekehard Olbrich, Nils Bertschinger, Nihat Ay, and Jürgen Jost, “How should complexity scale with system size?,” *The European Physical Journal B*, vol. 63, pp. 407–415, 2008.
- [16] Robin AA Ince, Bruno L Giordano, Christoph Kayser, Guillaume A Rousselet, Joachim Gross, and Philippe G Schyngs, “A statistical framework for neuroimaging data analysis based on mutual information estimated via a gaussian copula,” *Human brain mapping*, vol. 38, no. 3, pp. 1541–1573, 2017.
- [17] Jaroslav Hlinka, Milan Paluš, Martin Vejmelka, Dante Mantini, and Maurizio Corbetta, “Functional connectivity in resting-state fmri: is linear correlation sufficient?,” *Neuroimage*, vol. 54, no. 3, pp. 2218–2225, 2011.
- [18] Shujian Yu, Luis Gonzalo Sanchez Giraldo, Robert Jenssen, and Jose C Principe, “Multivariate extension of matrix-based renyi’s  $\alpha$ -order entropy functional,” *IEEE transactions on pattern analysis and machine intelligence*, vol. 42, no. 11, pp. 2960–2966, 2019.
- [19] Shujian Yu, Francesco Alesiani, Xi Yu, Robert Jenssen, and Jose Principe, “Measuring dependence with matrix-based entropy functional,” in *Proceedings of the AAAI Conference on Artificial Intelligence*, 2021, vol. 35, pp. 10781–10789.
- [20] Claude E Shannon, “A mathematical theory of communication,” *The Bell system technical journal*, vol. 27, no. 3, pp. 379–423, 1948.
- [21] Alfréd Rényi, “On measures of entropy and information,” in *Proceedings of the Fourth Berkeley Symposium on Mathematical Statistics and Probability, Volume 1: Contributions to the Theory of Statistics*. University of California Press, 1961, vol. 4, pp. 547–562.
- [22] Thomas M Cover and Joy A Thomas, “Information theory and statistics,” *Elements of information theory*, vol. 1, no. 1, pp. 279–335, 1991.
- [23] Luis Gonzalo Sanchez Giraldo, Murali Rao, and Jose C Principe, “Measures of entropy from data using infinitely divisible kernels,” *IEEE Transactions on Information Theory*, vol. 61, no. 1, pp. 535–548, 2014.
- [24] David Van Essen, Stephen Smith, Deanna Barch, Timothy Behrens, Essa Yacoub, and Kamil Ugurbil, “The wu-minn human connectome project: an overview,” *NeuroImage*, vol. 80, 05 2013.
- [25] Nathalie Tzourio-Mazoyer, Brigitte Landeau, Dimitri Papathanassiou, Fabrice Crivello, Octave Etard, Nicolas Delcroix, Bernard Mazoyer, and Marc Joliot, “Automated anatomical labeling of activations in spm using a macroscopic anatomical parcellation of the mni mri single-subject brain,” *Neuroimage*, vol. 15, no. 1, pp. 273–289, 2002.
- [26] Holmes CJ, Hoge R, Collins L, Woods R, Toga AW, and Evans AC, “Enhancement of mr images using registration for signal averaging,” *Journal of computer assisted tomography*, vol. 22, no. 2, pp. 324–333, 1998.
- [27] Andrea I Luppi, Pedro AM Mediano, Fernando E Rosas, Negin Holland, Tim D Fryer, John T O’Brien, James B Rowe, David K Menon, Daniel Bor, and Emmanuel A Stamatakis, “A synergistic core for human brain evolution and cognition,” *Nature Neuroscience*, vol. 25, no. 6, pp. 771–782, 2022.